

# EFFICIENT REPRESENTATION OF REALISTIC 3D STATIC MAGNETIC FIELDS FOR SYMPLECTIC TRACKING AND FIRST APPLICATIONS FOR FREQUENCY ANALYSIS AND DYNAMIC APERTURE STUDIES IN ELENA

Lajos Bojtár, CERN, Geneva, Switzerland

## Abstract

The algorithm called SIMPA has a new and unique approach to long-term 4D tracking of charged particles in arbitrary static electromagnetic fields. Field values given on the boundary of the region of interest are reproduced by an arrangement of hypothetical magnetic or electric point sources surrounding the boundary surface. The vector and scalar potentials are obtained by summing the contributions of each source. The second step of the method improves the evaluation speed of the potentials and their derivatives by orders of magnitude. This comprises covering the region of interest by overlapping spheres, then calculating the spherical harmonic expansion of the potentials on each sphere. During tracking, field values are evaluated by calculating the solid harmonics and their derivatives inside a sphere containing the particle. Frequency analysis and dynamic aperture studies in ELENA is presented. The effect of the end fields and the perturbation introduced by the magnetic system of the electron cooler on dynamic aperture is shown. The dynamic aperture calculated is the direct consequence of the geometry of the magnetic elements, no multipole errors have been added to the model.

## INTRODUCTION

In recent papers [1, 2] we described a new algorithm allowing long-term symplectic integration of charged particle trajectories in arbitrary static magnetic and electric fields. The approach to particle tracking we described naturally includes the end fields for all kinds of elements with the same treatment.

## THE TRACKING ALGORITHM

### *A Short Summary*

We recommend reading the previous papers [1, 2] to understand the algorithm in detail, as only a summary is provided here.

Symplectic integrators keep the conserved quantities bounded, but cannot cure the errors coming from the representation of the fields. These are two separate sources of errors. It is crucial to have a physically valid representation of the fields, otherwise there is a spurious energy drift during the tracking. The potentials are expressed analytically in terms of their sources. These sources are placed outside of the volume of interest, at some distance from the boundary, and their strength is set such that they reproduce the magnetic or electric field at the boundary by solving a system of linear equations. After the potentials are reproduced at the boundary by the sources, they can be evaluated analytically

anywhere inside the volume. However, this method is too slow to be practical.

Several orders of magnitude improvement can be achieved by using a local description of the potentials. Spherical harmonics scaled appropriately are called solid harmonics. Regular solid harmonics are the canonical representation for harmonic functions inside a sphere. A key characteristic of the algorithm is the description of vector and scalar potentials by solid harmonics inside a set of overlapping spheres covering the volume of interest.

The potentials satisfy exactly the Laplace equation inside the spheres. The discontinuity between the spheres decrease exponentially with the degree of solid harmonics expansion and can be easily kept close to machine precision. The representation of the potentials in terms of solid harmonics is optimal in terms of memory and allows fast evaluation.

The name of our software is SIMPA [3], an abbreviation of Symplectic Integration through MonoPole Arrangements. The workflow starts with modeling individual magnets with CAD software or measurement data, then the strengths of the point sources are calculated for each type of magnet. The next step is to assemble these sources according to the lattice of the machine. Finally, the solid harmonics coefficients of each sphere covering the volume of interest are calculated, providing a field map for the fast evaluation.

The boundary of the volume of interest is described by a Standard Tessellation Language (STL) file in SIMPA. The next step is to fill it with overlapping spheres, such that the entire beam region is covered without gaps. The spheres should be small enough to not overlap with the sources.

It is practical to place the center of the spheres onto a regular lattice. The coordinates of the sphere centers on an infinite HCP lattice can be obtained by three simple expressions. We keep only those spheres from the infinite lattice which are necessary to cover the beam region. Figure 1 shows the ELENA beam region and the centers of the covering spheres. The radius of the spheres was 1 cm in this study and about 76000 of them were needed to cover the aperture.

### *Preparing the Field Maps*

As a first step, the field of each type of magnet in ELENA has to be expressed as a collection of point sources. This provides continuous and analytic potential everywhere in the beam region. To do so, the magnetic field values have been obtained from the CAD software OPERA for each magnet at specific points on a surface surrounding the beam region. This surface is close to the poles of the magnet. The point sources are placed outside of the surface at 2.5 cm distance. Then a system of linear equation is solved to find

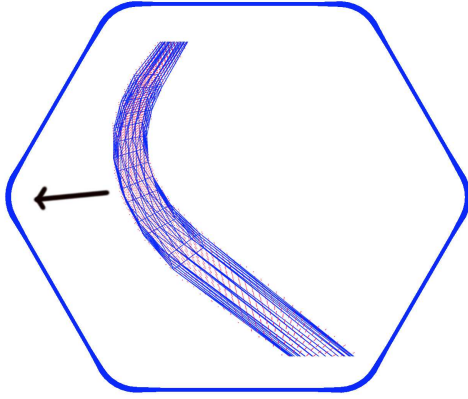


Figure 1: Triangulated boundary of the ELENA beam region. The interior plot is an expanded 3D view of an arc. The red dots are the centers of the covering spheres located on an HCP lattice.

the strengths of the point sources for each magnet type. The relative precision of the reproduction of the magnetic field from the vector potential is typically about  $10^{-3}$  in this study. The precision can be made better by increasing the number of point sources.

Once each type of magnet in the machine has been expressed as a collection of point sources, the next step is to assemble the ELENA ring from these collections. This is done by rotating and translating the collections of sources to the correct place.

The magnets of the ELENA ring have been organized into magnet families. Usually, a magnet family consists of magnets connected to the same power supply. For each magnet family, a field map was produced.

## FREQUENCY ANALYSIS

### The Method

The drift in the tunes can serve as an early indicator of the long-term stability of the motion [4]. For initial conditions corresponding to chaotic trajectories, the frequency can only be defined for a given time interval. Calculating this local frequency for two consecutive time intervals and taking their difference we can calculate tune shifts  $\Delta Q_{h,v}$ . For a coasting beam, the figure of merit can be defined as:

$$D = \log_{10}(\sqrt{\Delta Q_h^2 + \Delta Q_v^2}) \quad (1)$$

$D$  calculated with this definition can be used to identify stable areas in the tune diagram.

The tunes were scanned in 160 steps in both directions giving 25600 initial conditions. Each particle was tracked for 300 turns and the phase space variables were saved at a single longitudinal position for each turn. The tracking result is post-processed with PyNAFF, a Python implementation of the NAFF algorithm [5]. To calculate  $\Delta Q_{h,v}$ , we split the 300 turns into two sets. Then the figure of merit  $D$  in Eq.

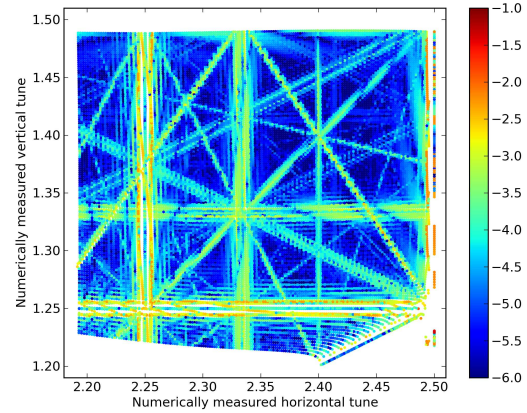


Figure 2:  $D$  plotted as colors against the numerically measured tunes for the bare ELENA machine, consisting of only the main bendings and the three quadrupole families.

(1) was calculated for each point in the diagram and plotted as colors.

### Results

Fig. 2 shows the figure of merit  $D$  for the bare ELENA machine with bending magnets and quadrupoles only, plotted against the tunes as colors. The exercise was repeated with the magnetic elements of the electron cooler included. Fig. 3 shows the numerically measured tunes with the electron cooler included. It is apparent that the magnets of the electron cooler have a significant effect on the beam dynamics. Many resonance lines became stronger and wider and particle losses are more frequent at the strongest resonance lines.

On both plots, many higher-order resonance lines can be seen. It should be emphasized, these resonance lines are present also in a perfectly manufactured, built, and aligned machine. We have not put any imperfections into the model. All the resonance lines are the results of the fringe fields of the bending magnets and the quadrupoles. They are the direct consequence of the geometry of the magnets.

## DYNAMIC APERTURE

The dynamic aperture of six working points has been calculated and displayed in Table 1 to compare resonance conditions with a non-resonant case. The selected set of tunes is indicated in Fig. 3. These resonance lines were selected because they are close to the region where the working point of ELENA was set during the commissioning. The first working point was chosen to be far from the strong resonance lines at  $Q_h = 2.455$ ,  $Q_v = 1.415$ . The other five points were placed on resonance lines with various orders.

Stability diagrams are given in Fig. 4 for each point in Fig. 3, which survived  $N = 10^4$  turns. In these diagrams, instead of the usual convention of using the physical beam dimensions in units of sigmas of the beam distribution on the axes, we used the single-particle emittances. We did so,

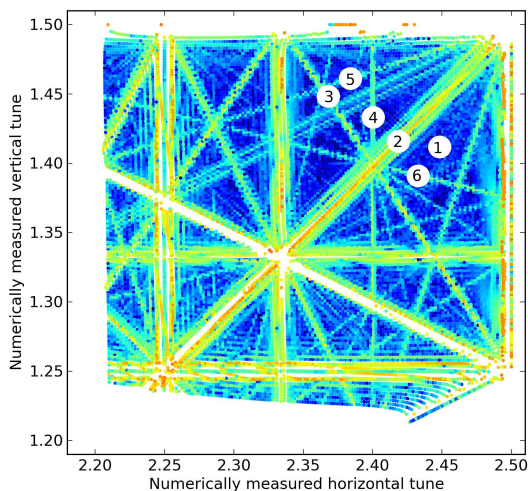


Figure 3:  $D$  plotted as colors on the same scale as above against the numerically measured tunes for the ELENA machine with the electron cooler included. The numbered white points in the tune diagram indicate the tunes where the dynamic aperture was calculated.

Table 1: Dynamic apertures  $r_d$  for the six points in Fig. 3 calculated with averaging over the dynamics, see [2].  $M$  is the angular grid size for  $r_d$  calculation.

| Point | $r_d$ [m] | $M$ | Resonance condition |
|-------|-----------|-----|---------------------|
| 1     | 0.0115    | 14  | NA                  |
| 2     | 0.012     | 8   | $Q_h - Q_v = 1$     |
| 3     | 0.01      | 6   | $3Q_h + 2Q_v = 10$  |
| 4     | 0.0117    | 3   | $5Q_h = 12$         |
| 5     | 0.0113    | 9   | $-Q_h + 3Q_v = 2$   |
| 6     | 0.0113    | 8   | $Q_h + 4Q_v = 8$    |

because in ELENA, the beam size depends on the performance and duration of the electron cooler, so there is no nominal emittance we could use for comparison.

In Fig. 4 it is apparent that some of the resonance lines make the dynamic aperture significantly smaller than the physical aperture. The transverse acceptance of ELENA is determined by the size of vacuum chambers and the optics.

## CONCLUSIONS

We have applied the SIMPA code for long-term symplectic charged particle tracking in arbitrary static electromagnetic fields on the ELENA machine.

The frequency and dynamic aperture analysis identified a number of 4th and 5th order resonance lines in the tune diagram strong enough to reduce the dynamic aperture below the physical one. What made the frequency and dynamic aperture analyses different, is the fact that we have not introduced any multipole error into our model apart from the

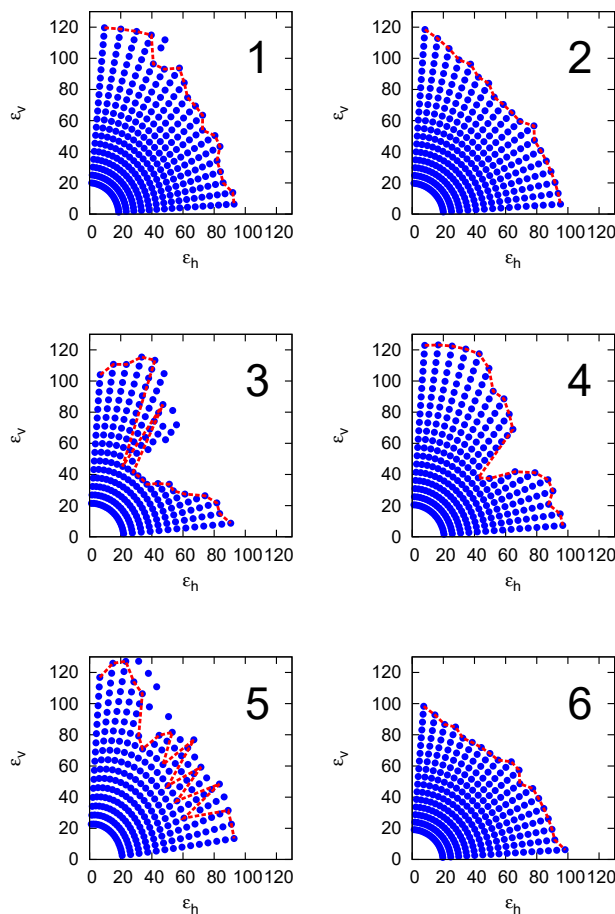


Figure 4: Initial emittances plotted in units of  $\pi$  mm mrad for particle with  $dp/p = 0$ . Only those initial conditions are plotted which survived  $N = 10^4$  turns. The numbers in the upper right corners correspond to the numbering in Fig. 3. The lines indicate the last connected initial emittances for each angle  $\alpha_k$ .

multipole components due to the geometry of the magnets, which are inevitable. All the resonances seen in the frequency analysis are direct consequences of the geometry of the fields, even if the magnetic elements are manufactured perfectly.

We showed in the frequency analysis section the effect of the magnetic system of the electron cooler on the beam dynamics by comparing the two cases, with and without electron cooler. The electron cooler introduced non-negligible magnetic perturbations, strengthening many resonance lines. To our best knowledge there was no similar study done before with electron coolers.

## ACKNOWLEDGMENTS

I would like to express my gratitude towards Gianluigi Arduini, Christian Carli, Massimo Giovannozzi and Lars Joergensen from CERN for their valuable comments and suggestions.

## REFERENCES

- [1] L. Bojtár. Efficient evaluation of arbitrary static electromagnetic fields with applications for symplectic particle tracking. *Nuclear Instruments and Methods A*, 948:162841, 2019. doi:10.1016/j.nima.2019.162841
- [2] Lajos Bojtár. Frequency analysis and dynamic aperture studies in a low energy antiproton ring with realistic 3D magnetic fields. *Phys. Rev. Accel. Beams*, 23:104002, Oct 2020. doi:10.1103/PhysRevAccelBeams.23.104002
- [3] <https://simpa-project.web.cern.ch/>.
- [4] E. Todesco, M. Giovannozzi, and W. Scandale. Fast indicators of long term stability. *Particle Accelerators*, 55:27–36, 1996.
- [5] F. Asvesta, N. Karastathis, and P. Zisopoulos. PyNAFF: A Python module that implements NAFF. <https://github.com/nkarast/PyNAFF>